Frontiers of Information Technology & Electronic Engineering
www.zju.edu.cn/jzus; engineering.cae.cn; www.springerlink.com
ISSN 2095-9184 (print); ISSN 2095-9230 (online)
E-mail: jzus@zju.edu.cn

Adaptive tracking control for air-breathing hypersonic vehicles with state constraints*

Gong-jun LI

(*Science and Technology on Space Intelligent Control Laboratory, Beijing Institute of Control Engineering, Beijing 100190, China*)

E-mail: gongjun_bice@buaa.edu.cn

Received Dec. 21, 2015; Revision accepted Feb. 26, 2016; Crosschecked Apr. 16, 2017

Abstract: We investigate the adaptive tracking problem for the longitudinal dynamics of state-constrained air-breathing hypersonic vehicles, where not only the velocity and the altitude, but also the angle of attack (AOA) is required to be tracked. A novel indirect AOA tracking strategy is proposed by viewing the pitch angle as a new output and devising an appropriate pitch angle reference trajectory. Then based on the redefined outputs (i.e., the velocity, the altitude, and the pitch angle), a modified backstepping design is proposed where the barrier Lyapunov function is used to solve the state-constrained control problem and the control gain of this class of systems is unknown. Stability analysis is given to show that the tracking objective is achieved, all the closed-loop signals are bounded, and all the states always satisfy the given constraints. Finally, numerical simulations verify the effectiveness of the proposed approach.

Key words: Hypersonic vehicle; Constraints; Output redefinition; Barrier Lyapunov function
http://dx.doi.org/10.1631/FITEE.1500464 **CLC number:** TP273; V448.2

1 Introduction

Air-breathing hypersonic vehicles (AHVs) are expected to play an indispensable role in future space transportation due to their high reliability and economic efficiency. Although there have been several successful flight tests from the US Air Force and NASA over past decades, the design of robust flight control systems for AHVs is still a challenging issue owing to significant couplings, nonlinearities, and uncertainties in the vehicle dynamics (Fidan *et al.*, 2003; Fiorentini and Serrani, 2012; Hu *et al.*, 2014a). Consequently, the study of flight control for AHVs attracts much attention from the aerospace community.

AHV dynamics with the winged-cone configuration was first proposed in Shaughnessy *et al.* (1990). Based on this dynamics, various results have been reported in the past 20 years (Gregory *et al.*, 1992; Fidan *et al.*, 2003; Xu HJ *et al.*, 2004; Xu B *et al.*, 2011; 2012; Li *et al.*, 2012; Sun HB *et al.*, 2013; Yang *et al.*, 2013; Wu *et al.*, 2014). It is noteworthy that Li *et al.* (2012) and Sun HB *et al.* (2013) considered the case of matched disturbances, while Yang *et al.* (2013) and Wu *et al.* (2014) considered the case of mismatched ones. A high-fidelity longitudinal model of an AHV similar to the configuration of X-30 and its simplified curve-fitted model (CFM) were proposed in Bolender and Doman (2007) and Parker *et al.* (2007), respectively. Because of the propulsion-airframe integration design, there exists strong coupling between the engine and the angle of attack (AOA) in a CFM, which makes the control for the CFM more challenging than that for the winged-cone configuration model. For an AHV, time delay may exist in flight control systems. Control of nonlinear time-delay systems has been a very active area

* Project supported by the National Natural Science Foundation of China (Nos. 61333008 and 61273153)
ORCID: Gong-jun LI, http://orcid.org/0000-0001-8503-2973

(Qiu *et al.*, 2015; Wang *et al.*, 2016). However, because of the heavy complexity of time-delay AHV dynamics, only a few results have been reported (Gibson *et al.*, 2009). Fuzzy sets and systems have attracted more and more attention for their universal approximation feature (Qiu *et al.*, 2013; 2016). Hu *et al.* (2014b) proposed a robust H_∞ dynamic output feedback controller by using a Takagi-Sugeno (T-S) fuzzy set to represent the AHV dynamics. Wu *et al.* (2014) proposed a fuzzy disturbance observer-based control (DOBC) design methodology for AHVs with modeled and unmodeled disturbances. For a CFM, the strong coupling between the engine and the AOA leads to the fact that the performance of air-breathing engines is very sensitive to the change of the AOA (Parker *et al.*, 2007; Mirmirani *et al.*, 2009). Therefore, it is necessary to force the AOA to track a given reference trajectory to improve the performance of air-breathing engines. However, to the best of our knowledge, the AOA is viewed only as an intermediate variable and its main role is to guarantee altitude tracking in the existing work (Fiorentini *et al.*, 2009; Sun HF *et al.*, 2013; Zong *et al.*, 2013). As a consequence, AOA tracking is difficult to achieve while ensuring altitude tracking.

In addition, the strong coupling between the engine and the AOA determines that the AOA must be strictly within a given envelope; otherwise, air-breathing engines will unstart and this phenomenon is unacceptable (Cox *et al.*, 1995). Thus, the control for AHVs with state constraints is of great importance. On state-constrained control of nonlinear systems, a large volume of results have been reported, e.g., invariance control (Wolff *et al.*, 2007; Burger and Guay, 2010), model predictive control (MPC) (Mayne *et al.*, 2000), reference governors (RG) (Bemporad, 1998; Gilbert and Kolmanovsky, 2002), barrier Lyapunov function (BLF) (Ngo *et al.*, 2005; Tee *et al.*, 2009; Tee and Ge, 2011; Liu *et al.*, 2014; Jin and Kwong, 2015), and the references therein. However, most of the existing results were derived based on strict assumptions on the controlled systems. For example, the control gain was assumed to be completely known for the BLF method with rare exceptions in Jin and Kwong (2015). For an AHV, these assumptions are not satisfied. For this reason, on the state-constrained control of AHVs, only a few results have been reported, derived by using the invariant set idea (Fiorentini *et al.*, 2009; Fiorentini and Serrani, 2012; Li and Meng, 2015). This idea includes two steps. First, a level set should be appropriately selected such that states satisfy a given constraint if error variables are within this level set. Second, a controller needs to be designed to ensure that this level set is an invariant set. In the two steps, the main challenge comes from the first step, which is still a trial-and-error procedure and thus a difficult task.

Motivated by the above, we study the adaptive tracking problem for the longitudinal dynamics of air-breathing hypersonic vehicles with state constraints, where not only the velocity and the altitude, but also the AOA is required to be tracked. Because the dynamics of the altitude and the AOA are affected by the same control action from aerodynamic control surfaces, simultaneous control of the altitude and the AOA essentially belongs to the field of underactuated control (Oland *et al.*, 2013; Pettersen, 2015). Underactuated control is a challenging issue in the control community. In addition, state-constrained control makes the problem even more complex. Consequently, we try to seek indirect AOA tracking by selecting the pitch angle as a new output and designing an appropriate pitch angle reference trajectory. Based on the redefined outputs (i.e., the velocity, the altitude, and the pitch angle), a modified backstepping design is proposed where the BLF method is used to cope with state constraints and the control gain of this class of systems is unknown. It is noteworthy that in this study, the conventional BLF (Ngo *et al.*, 2005; Tee *et al.*, 2009; Tee and Ge, 2011; Liu *et al.*, 2014) widely used is applied to the state-constrained control problem of nonlinear systems with unknown control gain. Moreover, a set of criteria is given, which guides the selection of reference trajectories and controller parameters. Compared with the existing work based on the invariant set idea (Fiorentini *et al.*, 2009; Fiorentini and Serrani, 2012; Li and Meng, 2015), the approach proposed makes the selection of controller parameters simpler.

Notations: In the subsequent sections, $\mathbf{0}_{m\times n}$ and $\boldsymbol{I}_p$ denote an $m\times n$ zero matrix and a $p\times p$ identity matrix, respectively. The symbols $(\cdot)_{\max}$ and $(\cdot)_{\min}$ denote the maximum and minimum values of '$\cdot$', respectively. For example, $(V_{\rm r})_{\max}$ denotes the maximum value of the velocity reference trajectory $V_{\rm r}$.

2 Vehicle model and control objective

The diagram of the longitudinal geometry profile and free body of an AHV in this study is depicted in Fig. 1. The longitudinal rigid dynamics are as follows (Serrani, 2013):

$$\dot{V} = \frac{T\cos\alpha - D}{m} - g\sin\gamma, \tag{1a}$$

$$\dot{h} = V\sin\gamma, \tag{1b}$$

$$\dot{\gamma} = \frac{L + T\sin\alpha}{mV} - \frac{g}{V}\cos\gamma, \tag{1c}$$

$$\dot{\theta}_{\rm p} = Q, \tag{1d}$$

$$\dot{Q} = \frac{M_{yy}}{I_{yy}}. \tag{1e}$$

Herein V, h, γ, $\theta_{\rm p}$, and Q denote the velocity, the altitude, the flight-path angle (FPA), the pitch angle, and the pitch rate, respectively; α denotes the AOA, which is defined as follows:

$$\alpha = \theta_{\rm p} - \gamma; \tag{2}$$

g denotes the acceleration of gravity; m and I_{yy} denote the vehicle mass and the moment of inertia, respectively; T, D, L, and M_{yy} denote the thrust, drag, lift, and pitching moment, respectively, whose curve-fit expressions are described as follows (Serrani, 2013):

$$T = \bar{q}S\left(C_{T,\varPhi}(\alpha)\varPhi + C_T(\alpha)\right), \tag{3a}$$

$$D = \bar{q}S\left(C_D^{\alpha^2}\alpha^2 + C_D^{\alpha}\alpha + C_D^0\right), \tag{3b}$$

$$L = \bar{q}S\left(C_L^{\alpha}\alpha + C_L^0 + C_L^{\delta_{\rm e}}\delta_{\rm e} + C_L^{\delta_{\rm c}}\delta_{\rm c}\right), \tag{3c}$$

$$M_{yy} = z_T T + \bar{q}S\bar{c}\left(C_M(\alpha) + C_M^{\delta_{\rm e}}\delta_{\rm e} + C_M^{\delta_{\rm c}}\delta_{\rm c}\right), \tag{3d}$$

where

$$C_{T,\varPhi}(\alpha) = C_{T,\varPhi}^{\alpha^3}\alpha^3 + C_{T,\varPhi}^{\alpha^2}\alpha^2 + C_{T,\varPhi}^{\alpha}\alpha + C_{T,\varPhi}^0,$$
$$C_T(\alpha) = C_T^{\alpha^3}\alpha^3 + C_T^{\alpha^2}\alpha^2 + C_T^{\alpha}\alpha + C_T^0,$$
$$C_M(\alpha) = C_M^{\alpha^2}\alpha^2 + C_M^{\alpha}\alpha + C_M^0.$$

Here, $\varPhi$, $\delta_{\rm e}$, and $\delta_{\rm c}$ denote the fuel equivalence ratio, the elevator angle, and the canard angle, respectively, which are the control inputs and affect the dynamics (Eqs. (1a)–(1e)) by T, L, and M_{yy}; $\bar{q}$ denotes the dynamic pressure; S, z_T, and $\bar{c}$ denote the reference area, the thrust moment arm, and the mean aerodynamic chord, respectively; the symbol C_i^j (e.g., $C_{T,\varPhi}^{\alpha^3}$, $C_M^{\alpha^2}$, and $C_M^{\delta_{\rm e}}$) denotes the aerodynamic coefficient. A detailed description of the dynamics can be found in Parker *et al.* (2007).

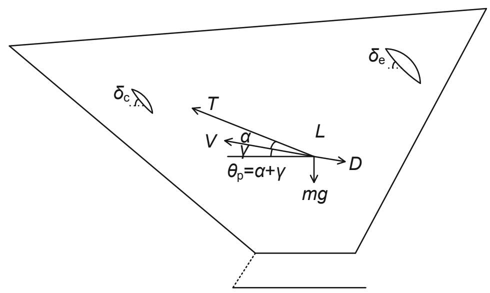

Fig. 1 Diagram of the longitudinal geometry profile and free body of an air-breathing hypersonic vehicle (Parker *et al.*, 2007; Bu *et al.*, 2016)

In this study, only the cruise phase is considered. For this phase, a flight envelope is shown in Table 1, which imposes some constraints on the states. Let $\mathcal{A}$ denote this flight envelope. We assume that all the inertial parameters (S, z_T, $\bar{c}$, m, and I_{yy}) and aerodynamic parameters (C_i^j) are unknown constants with $\pm10\%$ uncertainty tolerance, which yields the following uncertainty set:

$$\mathcal{P} = \{\boldsymbol{p} \in \mathbb{R}^n : 0.9p_i^0 \le p_i \le 1.1p_i^0,\ i = 1, 2, \ldots, n\}, \tag{4}$$

where p_i denotes an uncertain parameter, $\boldsymbol{p} = [p_1, p_2, \ldots, p_n]^{\rm T}$, n is the number of uncertain parameters, and p_i^0 denotes the nominal value of p_i.

Table 1 Admissible range, $\mathcal{A}$, for states (Parker *et al.*, 2007)

Variable	Minimum value	Maximum value
V (m/s)	2286	3352.8
h (m)	21 336	41 148
γ (deg)	−3	3
α (deg)	−5	10
$\theta_{\rm p}$ (deg)	−2	7
Q (deg/s)	−10	10

To ensure that the state-constrained control problem is solvable, define the following compact set $\mathcal{A}_1$ excluding the bounds of $\mathcal{A}$:

$$\mathcal{A}_1 = \{(V, h, \gamma, \theta_{\rm p}, Q) |\ \underline{j} \le j \le \overline{j},\ j = V, h, \gamma, \theta_{\rm p}, Q\}, \tag{5}$$

where $\underline{j}$ and $\overline{j}$ ($j = V$, h, γ, $\theta_{\rm p}$, Q) are known constants, satisfying

$$\begin{gathered}2286 \text{ m/s} < \underline{V} < \overline{V} < 3352.8 \text{ m/s},\\ 21\,336 \text{ m} < \underline{h} < \overline{h} < 41\,148 \text{ m},\\ -3 \text{ deg} < \underline{\gamma} < \overline{\gamma} < 3 \text{ deg},\\ -2 \text{ deg} < \underline{\theta}_{\mathrm{p}} < \overline{\theta}_{\mathrm{p}} < 7 \text{ deg},\\ -10 \text{ deg/s} < \underline{Q} < \overline{Q} < 10 \text{ deg/s}.\end{gathered}$$

Define $\boldsymbol{x} = [V, h, \gamma, \theta_{\mathrm{p}}, Q]^{\mathrm{T}}$, $\boldsymbol{u} = [\varPhi, \delta_{\mathrm{e}}, \delta_{\mathrm{c}}]^{\mathrm{T}}$, and $\boldsymbol{y} = [V, h, \alpha]^{\mathrm{T}}$. The control objective in this study is to design a control law $\boldsymbol{u}$, such that for any uncertain parameter vector $\boldsymbol{p} \in \mathcal{P}$, the output $\boldsymbol{y}$ tracks the reference trajectory $\boldsymbol{y}_{\mathrm{r}} = [V_{\mathrm{r}}, h_{\mathrm{r}}, \alpha_{\mathrm{r}}]^{\mathrm{T}}$ while ensuring that all the signals of the closed-loop system are bounded and that the state $\boldsymbol{x}$ is always within $\mathcal{A}$.

In this study, the following assumptions are made:

Assumption 1 For an arbitrary $t > 0$, V_{r}, $\dot{V}_{\mathrm{r}}$, h_{r}, $\dot{h}_{\mathrm{r}}$, $\ddot{h}_{\mathrm{r}}$, α_{r}, $\dot{\alpha}_{\mathrm{r}}$, and $\ddot{\alpha}_{\mathrm{r}}$ are known, smooth, and bounded, satisfying

$$\begin{cases}\underline{V} \le V_{\mathrm{r}}(t) \le \overline{V},\\ \underline{h} \le h_{\mathrm{r}}(t) \le \overline{h},\\ \underline{\theta}_{\mathrm{p}} \le \alpha_{\mathrm{r}}(t) \le \overline{\theta}_{\mathrm{p}},\end{cases}$$

where $\underline{V}$, $\overline{V}$, $\underline{h}$, $\overline{h}$, $\underline{\theta}_{\mathrm{p}}$, and $\overline{\theta}_{\mathrm{p}}$ are defined in Eq. (5).

Assumption 2 The initial state $\boldsymbol{x}(0) \in \mathcal{A}_1$.

From Assumptions 1 and 2, it can be seen that the initial states and the reference trajectories are always within $\mathcal{A}_1$ in this study. The main purpose of introducing the set $\mathcal{A}_1$ is to exclude the bounds of $\mathcal{A}$. Indeed, it is generally accepted to exclude the bounds of $\mathcal{A}$ to ensure that the state-constrained control problem is solvable (Tee *et al.*, 2009; Tee and Ge, 2011; Liu *et al.*, 2014), because the state constraint will be violated whenever the states reach the boundary of $\mathcal{A}$. Considering that we pursue indirect AOA tracking by selecting the pitch angle as a new output, thus it is assumed that $\underline{\theta}_{\mathrm{p}} \le \alpha_{\mathrm{r}}(t) \le \overline{\theta}_{\mathrm{p}}$ ($\forall\, t > 0$) in Assumption 1.

From Eq. (2) and Table 1, it can be seen that the AOA also satisfies the given constraint when the state $\boldsymbol{x}$ remains in $\mathcal{A}$.

3 Main results

3.1 Redefinition of outputs

In this subsection, the analysis indicates that direct AOA tracking is very difficult while ensuring altitude tracking. Therefore, an indirect AOA tracking idea is pursued by redefining the outputs.

In the system, there are three control inputs: $\varPhi$, δ_{e}, and δ_{c}. Among these control inputs, $\varPhi$ is used mainly to ensure $V - V_{\mathrm{r}} \to 0$. Hence, there are only two available inputs, i.e., δ_{e} and δ_{c}, to ensure $h - h_{\mathrm{r}} \to 0$ and $\alpha - \alpha_{\mathrm{r}} \to 0$. Differentiating Eq. (2) and using Eqs. (1c) and (1d) yield

$$\dot{\alpha} = Q - \frac{L + T\sin\alpha}{mV} + \frac{g}{V}\cos\gamma. \tag{6}$$

In addition, differentiating Eq. (1b) and using Eqs. (1a) and (1c) yield

$$\begin{aligned}\ddot{h} =& \left(\frac{T\cos\alpha - D}{m} - g\sin\gamma\right)\sin\gamma\\ &+ V\left(\frac{L + T\sin\alpha}{mV} - \frac{g}{V}\cos\gamma\right)\cos\gamma.\end{aligned} \tag{7}$$

From Eqs. (6) and (7), it can be seen that the same control action '$\bar{q}S\left(C_L^{\delta_{\mathrm{e}}}\delta_{\mathrm{e}} + C_L^{\delta_{\mathrm{c}}}\delta_{\mathrm{c}}\right)$' from L affects both h-dynamics and α-dynamics. As a consequence, it is very difficult to simultaneously ensure the tracking of the altitude and the AOA. In fact, simultaneous control of the altitude and the AOA belongs to the scope of underactuated control, which is a challenging issue in the control community. In this study, an indirect AOA tracking idea is proposed by selecting θ_{p} as a new output, and ensuring $V - V_{\mathrm{r}} \to 0$, $h - h_{\mathrm{r}} \to 0$, and $\theta_{\mathrm{p}} - \theta_{\mathrm{r}} \to 0$, where θ_{r} is a pitch angle reference trajectory to be designed.

Now, let us analyze how to design θ_{r}. Suppose that the velocity and the altitude have completely tracked their respective reference trajectories. From Eq. (1b), it is derived that $\gamma = \arcsin(\dot{h}_{\mathrm{r}}/V_{\mathrm{r}})$. Hence, the flight-path angle reference trajectory can be selected as $\gamma_{\mathrm{r}} = \arcsin(\dot{h}_{\mathrm{r}}/V_{\mathrm{r}})$. Furthermore, together with Eq. (2), the pitch angle reference trajectory can be selected as

$$\theta_{\mathrm{r}} = \alpha_{\mathrm{r}} + \arcsin(\dot{h}_{\mathrm{r}}/V_{\mathrm{r}}). \tag{8}$$

Similarly, to ensure that the state-constrained control problem is solvable, the following assumption is made:

Assumption 3 $\underline{\theta}_{\mathrm{p}} \le \theta_{\mathrm{r}} \le \overline{\theta}_{\mathrm{p}}$, where $\underline{\theta}_{\mathrm{p}}$ and $\overline{\theta}_{\mathrm{p}}$ are defined in Eq. (5).

3.2 Control law design

This subsection gives the controller design procedure. The dynamics (Eqs. (1a)–(1e)) can be divided into two functional subsystems: the velocity subsystem (Eq. (1a)) and the altitude subsystem (Eqs. (1b)–(1e)). The velocity subsystem is controlled by Φ, which affects this subsystem by T. The altitude subsystem is controlled by δ_e and δ_c, which affect this subsystem by L and M_{yy}. Next is the detailed design procedure. The stability results of the complete closed-loop system are presented in the subsequent subsection.

3.2.1 Control of the velocity subsystem

The velocity subsystem is described in Eq. (1a), where Φ is the control input. For this subsystem, our control objective is to ensure $V - V_\mathrm{r} \to 0$ and an adaptive dynamic inversion controller based on the BLF is proposed.

Define the velocity tracking error as

$$e_1 = V - V_\mathrm{r}. \tag{9}$$

Differentiating Eq. (9), and according to Eqs. (1a), (3a), and (3b), we have

$$\dot{e}_1 = \boldsymbol{\theta}_1^\mathrm{T} \left(f_1(\boldsymbol{x}) + g_1(\boldsymbol{x})\Phi\right) - \dot{V}_\mathrm{r}, \tag{10}$$

where

$$\begin{aligned} \boldsymbol{\theta}_1 = {} & \frac{S}{m}\Big[C_{T,\Phi}^{\alpha^3}, C_{T,\Phi}^{\alpha^2}, C_{T,\Phi}^{\alpha}, C_{T,\Phi}^{0}, C_{T}^{\alpha^3}, C_{T}^{\alpha^2}, \\ & C_T^{\alpha}, C_T^{0}, C_D^{\alpha^2}, C_D^{\alpha}, C_D^{0}, \frac{mg}{S}\Big]^\mathrm{T} \in \mathbb{R}^{12}, \\ g_1(\boldsymbol{x}) = {} & \bar{q}[\alpha^3\cos\alpha, \alpha^2\cos\alpha, \alpha\cos\alpha, \cos\alpha, \\ & \boldsymbol{0}_{1\times 8}]^\mathrm{T} \in \mathbb{R}^{12}, \\ f_1(\boldsymbol{x}) = {} & \bar{q}\Big[\boldsymbol{0}_{1\times 4}, \alpha^3\cos\alpha, \alpha^2\cos\alpha, \alpha\cos\alpha, \\ & \cos\alpha, -\alpha^2, -\alpha, -1, -\sin\gamma/\bar{q}\Big]^\mathrm{T} \in \mathbb{R}^{12}. \end{aligned}$$

It is easy to see that $\boldsymbol{\theta}_1$ is bounded for any uncertain parameter vector $\boldsymbol{p} \in \mathcal{P}$. Hence, a convex compact set Θ_1 is introduced which satisfies

$$\boldsymbol{\theta}_1 \in \Theta_1, \ \forall\, \boldsymbol{p} \in \mathcal{P}, \tag{11}$$

$$\boldsymbol{\vartheta}^\mathrm{T} g_1(\boldsymbol{x}) > \varrho_1 > 0, \ \forall\, \boldsymbol{\vartheta} \in \Theta_1, \ \forall\, \boldsymbol{x} \in \mathcal{A}, \tag{12}$$

where ϱ_1 is a positive constant. It should be noted that conditions (11) and (12) are easily satisfied for the uncertainty set $\mathcal{P}$ and the envelope $\mathcal{A}$ given in Eq. (4) and Table 1, respectively.

For Eq. (10), choose a Lyapunov function as

$$W_1(e_1, \tilde{\boldsymbol{\theta}}_1) = \frac{1}{2}\ln\frac{k_{b1}^2}{k_{b1}^2 - e_1^2} + \frac{1}{2}\tilde{\boldsymbol{\theta}}_1^\mathrm{T}\boldsymbol{\Gamma}_1^{-1}\tilde{\boldsymbol{\theta}}_1, \tag{13}$$

where k_{b1} is a positive constant to be determined in the subsequent stability analysis, $\boldsymbol{\Gamma}_1$ is a symmetric positive definite matrix, and $\tilde{\boldsymbol{\theta}}_1 \triangleq \hat{\boldsymbol{\theta}}_1 - \boldsymbol{\theta}_1$ denotes the error between $\boldsymbol{\theta}_1$ and its estimate $\hat{\boldsymbol{\theta}}_1$.

In Eq. (13), W_1 is called a barrier Lyapunov function (BLF) for two reasons: (1) W_1 is continuously differentiable and positive definite in the set $\Xi = \{|e_1| < \tau_1, \boldsymbol{\theta}_1 \in \Theta_1, \hat{\boldsymbol{\theta}}_1 \in \Theta_1\}$, where τ_1 is any positive constant satisfying $\tau_1 < k_{b1}$; (2) W_1 has the following feature:

$$W_1 \to +\infty, \text{ when } |e_1| < k_{b1} \text{ and } e_1 \to \pm k_{b1}.$$

W_1 can be viewed as a conventional BLF (Jin and Kwong, 2015) and it is widely used to solve the state-constrained control problem of nonlinear systems with completely known control gain (Ngo *et al.*, 2005; Tee *et al.*, 2009; Tee and Ge, 2011; Liu *et al.*, 2014). In this study, it is used to solve the state-constrained control problem of AHVs with unknown control gain.

According to the feature of W_1, if the initial state satisfies $|e_1(0)| < k_{b1}$ and W_1 is bounded, then it can be concluded that

$$|e_1(t)| < k_{b1}, \ \forall\, t > 0.$$

Furthermore, according to Eq. (9), it is clear that $V = e_1 + V_\mathrm{r}$. Therefore, if the following condition holds:

$$2286 \le (V_\mathrm{r})_{\min} - k_{b1} < (V_\mathrm{r})_{\max} + k_{b1} \le 3352.8,$$

it can be concluded that V satisfies the constraint $\mathcal{A}$ given in Table 1. In the above inequality, those numerical values such as 2286 and 3352.8 are from Table 1. Consequently, the key idea of controller design is to guarantee the boundedness of the BLF, which guides the controller design procedure throughout this study. From this point of view, the BLF method is an effective tool for solving the state-constrained control of nonlinear systems, even for those nonlinear systems based on fuzzy dynamic models (Qiu *et al.*, 2013).

In Eq. (13), calculating the time derivative of W_1 along trajectory (10) yields

$$\begin{aligned} \dot{W}_1 = {} & \frac{e_1}{k_{b1}^2 - e_1^2}\left(\boldsymbol{\theta}_1^\mathrm{T}\left(f_1(\boldsymbol{x}) + g_1(\boldsymbol{x})\Phi\right) - \dot{V}_\mathrm{r}\right) \\ & + \tilde{\boldsymbol{\theta}}_1^\mathrm{T}\boldsymbol{\Gamma}_1^{-1}\dot{\hat{\boldsymbol{\theta}}}_1. \end{aligned} \tag{14}$$

To guarantee the boundedness of W_1, select the certainty equivalent control law and the update law, respectively, as

$$\Phi = \frac{1}{\hat{\boldsymbol{\theta}}_1^{\mathrm{T}} g_1(\boldsymbol{x})} \left(-k_1 e_1 - \hat{\boldsymbol{\theta}}_1^{\mathrm{T}} f_1(\boldsymbol{x}) + \dot{V}_{\mathrm{r}} \right), \tag{15}$$

$$\dot{\hat{\boldsymbol{\theta}}}_1 = \mathrm{Proj}_{\hat{\boldsymbol{\theta}}_1 \in \Theta_1} \left\{ \boldsymbol{\Gamma}_1 \left[\frac{e_1}{k_{b1}^2 - e_1^2} \Big(f_1(\boldsymbol{x}) + g_1(\boldsymbol{x}) \Phi \Big) \right] \right\}, \tag{16}$$

where $k_1 > 0$ is a controller parameter and $\mathrm{Proj}_{\hat{\boldsymbol{\theta}}_1 \in \Theta_1}(\cdot)$ is a smooth projection operator (Krstic *et al.*, 1995) which is used to ensure the nonsingularity of the control law (15).

Substituting Eqs. (15) and (16) into Eq. (14) and using standard properties of the projection operator (Krstic *et al.*, 1995) yield

$$\dot{W}_1 \leq -k_1 \frac{e_1^2}{k_{b1}^2 - e_1^2}. \tag{17}$$

3.2.2 Control of the altitude subsystem

The altitude subsystem is described in Eqs. (1b)–(1e), where δ_{e} and δ_{c} are the control inputs which affect this subsystem by L and M_{yy}. Our control objective is to ensure $h - h_{\mathrm{r}} \to 0$ and $\theta_{\mathrm{p}} - \theta_{\mathrm{r}} \to 0$. Usually, in Eq. (3c), the lift from δ_{e} and δ_{c}, i.e., $\bar{q}S(C_L^{\delta_{\mathrm{e}}}\delta_{\mathrm{e}} + C_L^{\delta_{\mathrm{c}}}\delta_{\mathrm{c}})$, is very small, compared with the lift from the AOA, i.e., $\bar{q}S(C_L^{\alpha}\alpha + C_L^0)$. However, considering that h is slowly time-varying in the cruise flight phase, this small lift can be used to ensure $h - h_{\mathrm{r}} \to 0$. Meanwhile, the pitching moment from δ_{e} and δ_{c}, i.e., $\bar{q}S\bar{c}\left(C_M^{\delta_{\mathrm{e}}}\delta_{\mathrm{e}} + C_M^{\delta_{\mathrm{c}}}\delta_{\mathrm{c}}\right)$, is used to guarantee $\theta_{\mathrm{p}} - \theta_{\mathrm{r}} \to 0$. To clearly illustrate the controller design procedure, the altitude subsystem is further divided into two modules, i.e., (h, γ) module and (θ_{p}, Q) module. For the former, Eqs. (1b) and (1c) are considered and the aim is to ensure $h - h_{\mathrm{r}} \to 0$. For the latter, Eqs. (1d) and (1e) are considered and the aim is to ensure $\theta_{\mathrm{p}} - \theta_{\mathrm{r}} \to 0$. Next is the detailed design procedure.

1. (h, γ) module

For this module, Eqs. (1b) and (1c) are considered. By viewing the lift from δ_{e} and δ_{c} as the control input, an adaptive backstepping controller based on a BLF is proposed to ensure $h - h_{\mathrm{r}} \to 0$. Based on the backstepping idea (Krstic *et al.*, 1995), this design procedure includes two steps.

Step 1: Define the altitude tracking error as

$$e_2 = h - h_{\mathrm{r}}. \tag{18}$$

Differentiating e_2 with respect to time and using Eq. (1b) yield

$$\dot{e}_2 = V \sin\gamma - \dot{h}_{\mathrm{r}}. \tag{19}$$

By viewing γ as a virtual control input, introduce an error variable

$$e_3 = \gamma - \gamma_{\mathrm{d}}, \tag{20}$$

where γ_{d} is an ideal controller. Substituting Eq. (20) into Eq. (19) yields

$$\dot{e}_2 = V \sin\gamma_{\mathrm{d}} - \dot{h}_{\mathrm{r}} + 2V \cos\frac{\gamma + \gamma_{\mathrm{d}}}{2} \sin\frac{e_3}{2}. \tag{21}$$

Choose the following BLF:

$$W_2 = \frac{1}{2} \ln \frac{k_{b2}^2}{k_{b2}^2 - e_2^2}, \tag{22}$$

where k_{b2} is a positive constant to be determined in the subsequent stability analysis. The time derivative of W_2 along trajectory (21) is

$$\begin{aligned} \dot{W}_2 = & \frac{e_2}{k_{b2}^2 - e_2^2} \left(V \sin\gamma_{\mathrm{d}} - \dot{h}_{\mathrm{r}} \right) \\ & + 2V \frac{e_2}{k_{b2}^2 - e_2^2} \cos\frac{\gamma + \gamma_{\mathrm{d}}}{2} \sin\frac{e_3}{2}. \end{aligned} \tag{23}$$

For Eq. (23), γ_{d} is designed as

$$\gamma_{\mathrm{d}} = \arcsin\frac{-k_2 e_2 + \dot{h}_{\mathrm{r}}}{V}, \tag{24}$$

where $k_2 > 0$ is a controller parameter. Given that the 'arcsin' function is defined on $[-1, 1]$, the following inequality should hold:

$$-1 \leq \frac{-k_2 e_2(t) + \dot{h}_{\mathrm{r}}(t)}{V(t)} \leq 1, \ \forall\, t \geq 0.$$

From the proof process of Theorem 1 which is given in the subsequent subsection, it can be seen that V satisfies the constraint $\mathcal{A}$ and $|e_2(t)| < k_{b2}$ ($\forall\, t \geq 0$) if inequalities (53) and (54a)–(54e) hold. Together with inequalities (54a)–(54e), it can be further derived that

$$\left| \frac{-k_2 e_2(t) + \dot{h}_{\mathrm{r}}(t)}{V(t)} \right| < \frac{k_2 k_{b2} + |\dot{h}_{\mathrm{r}}|_{\max}}{2286} < 1, \ \forall\, t \geq 0.$$

Therefore, conditions (53) and (54a)–(54e) can ensure that γ_{d} is well-defined.

Substituting Eq. (24) into Eq. (23) yields

$$\dot{W}_2 = -k_2 \frac{e_2^2}{k_{b2}^2 - e_2^2} + 2V \frac{e_2}{k_{b2}^2 - e_2^2} \cos\frac{\gamma + \gamma_{\mathrm{d}}}{2} \sin\frac{e_3}{2}. \tag{25}$$

Here, the second term in the right side of Eq. (25), i.e., the coupling term, is canceled in the subsequent step.

Step 2 (final step): Substituting Eq. (20) into Eq. (1c) yields

$$\dot{e}_3 = \frac{L + T\sin\alpha}{mV} - \frac{g}{V}\cos\gamma - \dot{\gamma}_{\mathrm{d}}. \tag{26}$$

Now, let us calculate the term $\dot{\gamma}_{\mathrm{d}}$. Differentiating Eq. (24) and using Eqs. (1a), (18), and (1b) yield

$$\begin{aligned}\dot{\gamma}_{\mathrm{d}} =& \varDelta_1\left(\frac{-k_2(V\sin\gamma - \dot{h}_{\mathrm{r}}) + \ddot{h}_{\mathrm{r}}}{V}\right. \\ &\left.-\frac{(-k_2e_2 + \dot{h}_{\mathrm{r}})\dot{V}}{V^2}\right) \\ =& \varDelta_1\left(\frac{-k_2(V\sin\gamma - \dot{h}_{\mathrm{r}}) + \ddot{h}_{\mathrm{r}}}{V}\right. \\ &\left.-\frac{-k_2e_2 + \dot{h}_{\mathrm{r}}}{V^2}\left(\frac{T\cos\alpha - D}{m} - g\sin\gamma\right)\right) \\ =& \varDelta_1\left(-\frac{-k_2e_2 + \dot{h}_{\mathrm{r}}}{V^2}\cdot\frac{T\cos\alpha - D}{m}\right. \\ &\left.+\frac{-k_2e_2 + \dot{h}_{\mathrm{r}}}{V^2}g\sin\gamma + \varDelta_2\right),\end{aligned} \tag{27}$$

where $\varDelta_i$ $(i = 1, 2)$ are defined as

$$\begin{aligned}\varDelta_1 =& 1\bigg/\sqrt{1 - \left(\frac{-k_2e_2 + \dot{h}_{\mathrm{r}}}{V}\right)^2}, \\ \varDelta_2 =& \frac{-k_2(V\sin\gamma - \dot{h}_{\mathrm{r}}) + \ddot{h}_{\mathrm{r}}}{V}.\end{aligned}$$

Clearly, $\varDelta_i$ $(i = 1, 2)$ do not include any uncertain parameter.

Substituting Eq. (27) into Eq. (26) yields

$$\begin{aligned}\dot{e}_3 =& \frac{L + T\sin\alpha}{mV} - \frac{g}{V}\cos\gamma \\ &+ \varDelta_1\frac{-k_2e_2 + \dot{h}_{\mathrm{r}}}{V^2}\cdot\frac{T\cos\alpha - D}{m} \\ &- \varDelta_1\frac{-k_2e_2 + \dot{h}_{\mathrm{r}}}{V^2}g\sin\gamma - \varDelta_1\varDelta_2.\end{aligned} \tag{28}$$

Substituting Eqs. (3a)–(3c) into Eq. (28) further yields

$$\dot{e}_3 = \boldsymbol{\theta}_2^{\mathrm{T}}[f_2(\boldsymbol{x}) + g_2(\boldsymbol{x})\boldsymbol{U}_\delta] - \varDelta_1\varDelta_2, \tag{29}$$

where

$$\left\{\begin{aligned}&\boldsymbol{\theta}_2 = \frac{S}{m}\Big[C_L^{\delta_{\mathrm{e}}}, C_L^{\delta_{\mathrm{c}}}, C_{T,\varPhi}^{\alpha^3}, C_{T,\varPhi}^{\alpha^2}, C_{T,\varPhi}^{\alpha}, C_{T,\varPhi}^{0}, \\ &\qquad C_T^{\alpha^3}, C_T^{\alpha^2}, C_T^{\alpha}, C_T^{0}, C_D^{\alpha^2}, C_D^{\alpha}, C_D^{0}, \\ &\qquad C_L^{\alpha}, C_L^{0}, \frac{mg}{S}\Big]^{\mathrm{T}} \in \mathbb{R}^{16}, \\ &f_2(\boldsymbol{x}) = \frac{\bar{q}}{V}\Big[0, 0, \varPhi\alpha^3\varDelta_3, \varPhi\alpha^2\varDelta_3, \varPhi\alpha\varDelta_3, \varPhi\varDelta_3, \\ &\qquad \alpha^3\varDelta_3, \alpha^2\varDelta_3, \alpha\varDelta_3, \varDelta_3, \\ &\qquad \alpha^2\varDelta_4, \alpha\varDelta_4, \varDelta_4, \alpha, 1, \varDelta_5\Big]^{\mathrm{T}} \in \mathbb{R}^{16}, \\ &g_2(\boldsymbol{x}) = \frac{\bar{q}}{V}\left[\boldsymbol{I}_2,\ \boldsymbol{0}_{2\times14}\right]^{\mathrm{T}} \in \mathbb{R}^{16\times2}, \\ &\boldsymbol{U}_\delta = [\delta_{\mathrm{e}}, \delta_{\mathrm{c}}]^{\mathrm{T}}, \\ &\varDelta_3 = \sin\alpha + \varDelta_1\frac{(-k_2e_2 + \dot{h}_{\mathrm{r}})\cos\alpha}{V}, \\ &\varDelta_4 = -\varDelta_1\frac{-k_2e_2 + \dot{h}_{\mathrm{r}}}{V}, \\ &\varDelta_5 = -\frac{\cos\gamma}{V} - \varDelta_1\frac{-k_2e_2 + \dot{h}_{\mathrm{r}}}{V^2}\sin\gamma.\end{aligned}\right. \tag{30}$$

Similar to the former analysis, a convex compact set $\varTheta_2$ is introduced to cover all the values of $\boldsymbol{\theta}_2$, i.e., $\boldsymbol{\theta}_2 \in \varTheta_2$.

Choose the following BLF:

$$W_3 = W_2 + \frac{1}{2}\ln\frac{k_{b3}^2}{k_{b3}^2 - e_3^2} + \frac{1}{2}\tilde{\boldsymbol{\theta}}_2^{\mathrm{T}}\boldsymbol{\varGamma}_2^{-1}\tilde{\boldsymbol{\theta}}_2, \tag{31}$$

where W_2 is defined in Eq. (22), k_{b3} is a positive constant to be determined in the subsequent stability analysis, $\boldsymbol{\varGamma}_2 > 0$ is a symmetric positive definite matrix, and $\tilde{\boldsymbol{\theta}}_2 \triangleq \hat{\boldsymbol{\theta}}_2 - \boldsymbol{\theta}_2$ denotes the error between $\boldsymbol{\theta}_2$ and its estimate $\hat{\boldsymbol{\theta}}_2$.

In Eq. (31), differentiating W_3 with respect to time and using Eqs. (25) and (29) yield

$$\begin{aligned}\dot{W}_3 =& -k_2\frac{e_2^2}{k_{b2}^2 - e_2^2} + 2V\frac{e_2}{k_{b2}^2 - e_2^2}\cos\frac{\gamma + \gamma_{\mathrm{d}}}{2}\sin\frac{e_3}{2} \\ &+ \frac{e_3}{k_{b3}^2 - e_3^2}\left(\boldsymbol{\theta}_2^{\mathrm{T}}[f_2(\boldsymbol{x}) + g_2(\boldsymbol{x})\boldsymbol{U}_\delta] - \varDelta_1\varDelta_2\right) \\ &+ \tilde{\boldsymbol{\theta}}_2^{\mathrm{T}}\boldsymbol{\varGamma}_2^{-1}\dot{\hat{\boldsymbol{\theta}}}_2.\end{aligned} \tag{32}$$

To guarantee the boundedness of W_3, select the certainty equivalent control law and the update law, respectively, as

$$\begin{aligned}\hat{\boldsymbol{\theta}}_2^{\mathrm{T}}(f_2(\boldsymbol{x}) + g_2(\boldsymbol{x})\boldsymbol{U}_\delta) =& -k_3e_3 + \varDelta_1\varDelta_2 \\ &- Ve_2\frac{k_{b3}^2 - e_3^2}{k_{b2}^2 - e_2^2}\cos\frac{\gamma + \gamma_{\mathrm{d}}}{2}\cdot\frac{\sin(e_3/2)}{e_3/2},\end{aligned} \tag{33}$$

$$\dot{\hat{\boldsymbol{\theta}}}_2 = \mathrm{Proj}_{\hat{\boldsymbol{\theta}}_2 \in \varTheta_2}\left\{\boldsymbol{\varGamma}_2\frac{e_3}{k_{b3}^2 - e_3^2}\left[f_2(\boldsymbol{x}) + g_2(\boldsymbol{x})\boldsymbol{U}_\delta\right]\right\}, \tag{34}$$

where $k_3 > 0$ is a controller parameter and $\mathrm{Proj}_{\hat{\boldsymbol{\theta}}_2\in\Theta_2}(\cdot)$ is a smooth projection operator (Krstic *et al.*, 1995). It should be noted that in Eq. (33) the term ' $\sin(\cdot)/(\cdot)$ ' is defined as

$$\frac{\sin\eta}{\eta}=\begin{cases}1, & \eta=0,\\ \dfrac{\sin\eta}{\eta}, & \text{otherwise.}\end{cases}$$

Therefore, the term '$\sin(\cdot)/(\cdot)$' is always nonsingular.

Substituting Eqs. (33) and (34) into Eq. (32) and using standard properties of the projection operator (Krstic *et al.*, 1995) yield

$$\dot{W}_3\leq -k_2\frac{e_2^2}{k_{b2}^2-e_2^2}-k_3\frac{e_3^2}{k_{b3}^2-e_3^2}. \tag{35}$$

2. (θ_p, Q) module

For this module, Eqs. (1d) and (1e) are considered. By viewing the pitching moment from δ_e and δ_c as the control input, an adaptive backstepping controller based on a BLF is proposed to ensure $\theta_\mathrm{p}-\theta_\mathrm{r}\to 0$. Similar to the (h,γ) module, this design procedure includes two steps.

Step 1: Define the pitch angle tracking error as

$$e_4=\theta_\mathrm{p}-\theta_\mathrm{r}. \tag{36}$$

Substituting Eq. (36) into Eq. (1d) yields

$$\dot{e}_4=Q-\dot{\theta}_\mathrm{r}. \tag{37}$$

By viewing Q as a virtual control input, introduce an error variable

$$e_5=Q-Q_\mathrm{d}, \tag{38}$$

where Q_d is an ideal controller. Substituting Eq. (38) into Eq. (37) yields

$$\dot{e}_4=Q_\mathrm{d}-\dot{\theta}_\mathrm{r}+e_5. \tag{39}$$

Choose the following BLF:

$$W_4=\frac{1}{2}\ln\frac{k_{b4}^2}{k_{b4}^2-e_4^2}, \tag{40}$$

where k_{b4} is a positive constant to be determined in the subsequent stability analysis. The time derivative of W_4 along trajectory (39) is

$$\dot{W}_4=\frac{e_4}{k_{b4}^2-e_4^2}\left(Q_\mathrm{d}-\dot{\theta}_\mathrm{r}\right)+\frac{e_4}{k_{b4}^2-e_4^2}e_5. \tag{41}$$

For Eq. (41), Q_d is designed as follows:

$$Q_\mathrm{d}=-k_4e_4+\dot{\theta}_\mathrm{r}, \tag{42}$$

where $k_4>0$ is a controller parameter. Substituting Eq. (42) into Eq. (41) yields

$$\dot{W}_4=-k_4\frac{e_4^2}{k_{b4}^2-e_4^2}+\frac{e_4}{k_{b4}^2-e_4^2}e_5. \tag{43}$$

Here, the coupling term '$e_4e_5/(k_{b4}^2-e_4^2)$' is canceled in the subsequent step.

Step 2 (final step): Substituting Eq. (38) into Eq. (1e) yields

$$\dot{e}_5=M_{yy}/I_{yy}-\dot{Q}_\mathrm{d}. \tag{44}$$

Differentiating Eq. (42) and using Eq. (37) lead to $\dot{Q}_\mathrm{d}=-k_4(Q-\dot{\theta}_\mathrm{r})+\ddot{\theta}_\mathrm{r}$.

Substituting Eq. (3d) into Eq. (44) yields

$$\dot{e}_5=\boldsymbol{\theta}_3^\mathrm{T}(f_3(\boldsymbol{x})+g_3(\boldsymbol{x})\boldsymbol{U}_\delta)-\dot{Q}_\mathrm{d}, \tag{45}$$

where $\boldsymbol{U}_\delta$ is defined in Eq. (30), and $\boldsymbol{\theta}_3$, $f_3(\boldsymbol{x})$, and $g_3(\boldsymbol{x})$ are defined as follows:

$$\begin{aligned}\boldsymbol{\theta}_3=&\frac{S}{I_{yy}}\Big[\bar{c}C_M^{\delta_\mathrm{e}},\bar{c}C_M^{\delta_\mathrm{c}},z_TC_{T,\Phi}^{\alpha^3},z_TC_{T,\Phi}^{\alpha^2},z_TC_{T,\Phi}^{\alpha},\\&z_TC_{T,\Phi}^{0},z_TC_{T}^{\alpha^3},\left(z_TC_T^{\alpha^2}+\bar{c}C_M^{\alpha^2}\right),\\&(z_TC_T^{\alpha}+\bar{c}C_M^{\alpha}),(z_TC_T^{0}+\bar{c}C_M^{0})\Big]^\mathrm{T}\in\mathbb{R}^{10},\\f_3(\boldsymbol{x})=&\bar{q}\Big[0,0,\alpha^3\Phi,\alpha^2\Phi,\alpha\Phi,\Phi,\alpha^3,\alpha^2,\alpha,1\Big]^\mathrm{T}\in\mathbb{R}^{10},\\g_3(\boldsymbol{x})=&\bar{q}\left[\boldsymbol{I}_2,\boldsymbol{0}_{2\times 8}\right]^\mathrm{T}\in\mathbb{R}^{10\times 2}.\end{aligned}$$

Similar to the former analysis, here a convex compact set Θ_3 is introduced to cover all the values of $\boldsymbol{\theta}_3$, i.e., $\boldsymbol{\theta}_3\in\Theta_3$.

Choose the following BLF:

$$W_5=W_4+\frac{1}{2}\ln\frac{k_{b5}^2}{k_{b5}^2-e_5^2}+\frac{1}{2}\tilde{\boldsymbol{\theta}}_3^\mathrm{T}\boldsymbol{\Gamma}_3^{-1}\tilde{\boldsymbol{\theta}}_3, \tag{46}$$

where W_4 is defined in Eq. (40), k_{b5} is a positive constant to be determined in the subsequent stability analysis, $\boldsymbol{\Gamma}_3>0$ is a symmetric positive definite matrix, and $\tilde{\boldsymbol{\theta}}_3\triangleq\hat{\boldsymbol{\theta}}_3-\boldsymbol{\theta}_3$ denotes the error between $\boldsymbol{\theta}_3$ and its estimate $\hat{\boldsymbol{\theta}}_3$.

In Eq. (46), differentiating W_5 with respect to time and using Eqs. (43) and (45) yield

$$\begin{aligned}\dot{W}_5=&-k_4\frac{e_4^2}{k_{b4}^2-e_4^2}+\frac{e_4}{k_{b4}^2-e_4^2}e_5+\tilde{\boldsymbol{\theta}}_3^\mathrm{T}\boldsymbol{\Gamma}_3^{-1}\dot{\hat{\boldsymbol{\theta}}}_3\\&+\frac{e_5}{k_{b5}^2-e_5^2}\left(\boldsymbol{\theta}_3^\mathrm{T}(f_3(\boldsymbol{x})+g_3(\boldsymbol{x})\boldsymbol{U}_\delta)-\dot{Q}_\mathrm{d}\right).\end{aligned} \tag{47}$$

To guarantee the boundedness of W_5, select the certainty equivalent control law and the update law, respectively, as

$$\hat{\boldsymbol{\theta}}_3^{\mathrm{T}}(f_3(\boldsymbol{x})+g_3(\boldsymbol{x})\boldsymbol{U}_\delta)=-k_5e_5-e_4\frac{k_{b5}^2-e_5^2}{k_{b4}^2-e_4^2}+\dot{Q}_{\mathrm{d}}, \tag{48}$$

$$\dot{\hat{\boldsymbol{\theta}}}_3=\mathrm{Proj}_{\hat{\boldsymbol{\theta}}_3\in\Theta_3}\left\{\boldsymbol{\varGamma}_3\frac{e_5}{k_{b5}^2-e_5^2}[f_3(\boldsymbol{x})+g_3(\boldsymbol{x})\boldsymbol{U}_\delta]\right\}, \tag{49}$$

where $k_5>0$ is a controller parameter and $\mathrm{Proj}_{\hat{\boldsymbol{\theta}}_3\in\Theta_3}(\cdot)$ is a smooth projection operator (Krstic *et al.*, 1995).

Substituting Eqs. (48) and (49) into Eq. (47) and using standard properties of the projection operator (Krstic *et al.*, 1995) yield

$$\dot{W}_5\leq -k_4\frac{e_4^2}{k_{b4}^2-e_4^2}-k_5\frac{e_5^2}{k_{b5}^2-e_5^2}. \tag{50}$$

Finally, solving Eqs. (33) and (48) yields the actual control law for the control surfaces:

$$\begin{aligned}\boldsymbol{U}_\delta=\begin{bmatrix}\delta_{\mathrm{e}}\\ \delta_{\mathrm{c}}\end{bmatrix}&=\boldsymbol{B}^{-1}\Big[-k_3e_3+\Delta_1\Delta_2-\hat{\boldsymbol{\theta}}_2^{\mathrm{T}}f_2(\boldsymbol{x})\\ &-Ve_2\frac{k_{b3}^2-e_3^2}{k_{b2}^2-e_2^2}\cos\frac{\gamma+\gamma_{\mathrm{d}}}{2}\cdot\frac{\sin(e_3/2)}{e_3/2},\ -k_5e_5\\ &-e_4\frac{k_{b5}^2-e_5^2}{k_{b4}^2-e_4^2}+\dot{Q}_{\mathrm{d}}-\hat{\boldsymbol{\theta}}_3^{\mathrm{T}}f_3(\boldsymbol{x})\Big]^{\mathrm{T}},\end{aligned} \tag{51}$$

where $\boldsymbol{B}=\begin{bmatrix}\hat{\boldsymbol{\theta}}_2^{\mathrm{T}}g_2(\boldsymbol{x})\\ \hat{\boldsymbol{\theta}}_3^{\mathrm{T}}g_3(\boldsymbol{x})\end{bmatrix}$.

From Eq. (51), it can be seen that the smooth parameter projections in Eqs. (34) and (49) are used to ensure the nonsingularity of matrix $\boldsymbol{B}$. To this end, the convex compact set Θ_i ($i=2$, 3) should be appropriately selected such that

$$|\det(\boldsymbol{B})|>\varrho_2>0,\ \forall\,\boldsymbol{x}\in\mathcal{A},\ \forall\,\hat{\boldsymbol{\theta}}_i\in\Theta_i,\ i=2,3, \tag{52}$$

where $\det(\boldsymbol{B})$ denotes the determinant of $\boldsymbol{B}$ and ϱ_2 is a constant. Note that condition (52) is easily satisfied for the uncertainty set $\mathcal{P}$ and the envelope $\mathcal{A}$ given in Eq. (4) and Table 1, respectively.

Remark 1 From Eqs. (33) and (48), it can be observed that δ_{e} and δ_{c} play the same role in this study. On the one hand, they force the altitude to track the altitude reference trajectory by the lift from δ_{e} and δ_{c}. On the other hand, they force the pitch angle to track the pitch angle reference trajectory by the pitching moment from δ_{e} and δ_{c}.

3.3 Performance analysis of the closed-loop system

This subsection gives the stability results, which can be described as the following theorem:

Theorem 1 Under Assumptions 1–3, consider the closed-loop system consisting of the plant (Eqs. (1a)–(3d)), the control laws (Eqs. (15) and (51)), and the update laws (Eqs. (16), (34), and (49)). If there exist constants $k_i>0$ and $k_{bj}>0$ ($i,j=1$, 2, …, 5) such that

(C1) the initial state $\boldsymbol{x}(0)$ satisfies

$$|e_s(0)|<k_{bs},\ s=1,2,\ldots,5, \tag{53}$$

(C2) the following inequalities hold:

$$2286\leq(V_{\mathrm{r}})_{\min}-k_{b1}<(V_{\mathrm{r}})_{\max}+k_{b1}\leq 3352.8, \tag{54a}$$

$$21\,336\leq(h_{\mathrm{r}})_{\min}-k_{b2}<(h_{\mathrm{r}})_{\max}+k_{b2}\leq 41\,148, \tag{54b}$$

$$k_{b3}+\arcsin\Big((k_2k_{b2}+|\dot{h}_{\mathrm{r}}|_{\max})/2286\Big)\leq 3\pi/180, \tag{54c}$$

$$-2\pi/180\leq(\theta_{\mathrm{r}})_{\min}-k_{b4}<(\theta_{\mathrm{r}})_{\max}+k_{b4}\leq 7\pi/180, \tag{54d}$$

$$\begin{aligned}-10\pi/180\leq(\dot{\theta}_{\mathrm{r}})_{\min}-k_{b5}-k_4k_{b4}<(\dot{\theta}_{\mathrm{r}})_{\max}\\ +k_{b5}+k_4k_{b4}\leq 10\pi/180,\end{aligned} \tag{54e}$$

then for any uncertain parameter vector $\boldsymbol{p}\in\mathcal{P}$, the following properties hold:

(i) $\boldsymbol{x}(t)\in\mathcal{A}$, $\forall\,t\geq 0$;

(ii) all the closed-loop signals are bounded;

(iii) $\boldsymbol{y}(t)-\boldsymbol{y}_{\mathrm{r}}(t)\to\boldsymbol{0}$, as $t\to\infty$.

In inequalities (54a)–(54e), the numerical values such as 2286 and 3352.8 are from Table 1.

Proof Choose the following Lyapunov function:

$$W=W_1+W_3+W_5, \tag{55}$$

where W_1, W_3, and W_5 are defined in Eqs. (13), (31), and (46), respectively. Differentiating W with respect to time and using inequalities (17), (35), and (50) yield

$$\dot{W}\leq-\sum_{i=1}^{5}k_i\frac{e_i^2}{k_{bi}^2-e_i^2}. \tag{56}$$

Therefore, it is clear that $\dot{W}\leq 0$ in the set $\Omega=\{|e_i|<k_{bi},\ i=1,2,\ldots,5\}$, which means that W is monotonously non-increasing in Ω. Based on inequality (53), it is further derived that $W(t)\leq W(0)$,

$\forall\, t > 0$. According to the definition of W in Eq. (55) and using Eqs. (13), (31), and (46), it can be concluded that there exists constant $\varsigma_i > 0$ such that $|e_i| < \varsigma_i < k_{bi}$ $(i = 1, 2, \ldots, 5)$.

1. Proof of property (i)

First, let us prove that V, h, and θ_{p} satisfy the constraint $\mathcal{A}$. From Eq. (9), it is clear that $V = e_1 + V_{\mathrm{r}}$. By using $|e_1| < k_{b1}$ and inequality (54a), it is further derived that V satisfies the constraint $\mathcal{A}$. Similarly, h and θ_{p} satisfy the constraint $\mathcal{A}$. Second, let us prove that Q satisfies the constraint $\mathcal{A}$. From Eqs. (38) and (42), it is clear that $Q = e_5 - k_4 e_4 + \dot{\theta}_{\mathrm{r}}$. Together with $|e_i| < k_{bi}$ $(i = 4, 5)$ and using inequality (54e), it can be concluded that Q satisfies the constraint $\mathcal{A}$. Finally, let us prove that γ satisfies the constraint $\mathcal{A}$. From Eqs. (20) and (24), it is clear that

$$\gamma = e_3 + \arcsin\Big(\big(-k_2 e_2 + \dot{h}_{\mathrm{r}}\big)/V\Big).$$

Given that V satisfies the constraint $\mathcal{A}$ and $|e_i| < k_{bi}$ $(i = 2, 3)$, and using inequality (54c), it is derived that

$$|\gamma| \le k_{b3} + \arcsin\Big((k_2 k_{b2} + |\dot{h}_{\mathrm{r}}|_{\max})/2286\Big) \le 3\pi/180.$$

Therefore, γ satisfies the constraint $\mathcal{A}$. In other words, we have proved property (i).

2. Proof of property (ii)

First, according to property (i), $\boldsymbol{x}$ is obviously bounded. Second, using standard properties of the projection operator (Krstic *et al.*, 1995), the estimate $\hat{\boldsymbol{\theta}}_i$ of $\boldsymbol{\theta}_i$ $(i = 1, 2, 3)$ is bounded. Finally, let us prove the boundedness of $\boldsymbol{u}$, which is given in Eqs. (15) and (51). Given that $\boldsymbol{x}$ and $\hat{\boldsymbol{\theta}}_i$ $(i = 1, 2, 3)$ are bounded and $|e_i| < \varsigma_i < k_{bi}$ $(i = 1, 2, \ldots, 5)$, and using inequalities (12) and (52), it can be concluded that $\boldsymbol{u}$ is bounded. Hence, we have proved property (ii).

3. Proof of property (iii)

Considering inequality (56) and using $|e_i| < k_{bi}$ $(i = 1, 2, \ldots, 5)$, it is derived that

$$\dot{W} \le -\sum_{i=1}^{5} \frac{k_i}{k_{bi}^2} e_i^2. \tag{57}$$

By LaSalle's invariance principle (Slotine and Li, 1991), it can be concluded that $e_i \to 0$ $(i = 1, 2, \ldots, 5)$. On the one hand, $e_1 \to 0$ and $e_2 \to 0$ indicate $V - V_{\mathrm{r}} \to 0$ and $h - h_{\mathrm{r}} \to 0$, respectively. On the other hand, using Eqs. (2), (36), (20), (8), and (24), it is clear that

$$\begin{aligned} \alpha - \alpha_{\mathrm{r}} &= \theta_{\mathrm{p}} - \gamma - \alpha_{\mathrm{r}} \\ &= (\theta_{\mathrm{p}} - \theta_{\mathrm{r}}) - (\gamma - \gamma_{\mathrm{d}}) - \alpha_{\mathrm{r}} + \theta_{\mathrm{r}} - \gamma_{\mathrm{d}} \\ &= e_4 - e_3 + \beta_1 - \beta_2, \end{aligned} \tag{58}$$

where $\beta_1 = \arcsin\dfrac{\dot{h}_{\mathrm{r}}}{V_{\mathrm{r}}}$ and $\beta_2 = \arcsin\dfrac{-k_2 e_2 + \dot{h}_{\mathrm{r}}}{V}$. Given that V and V_{r} satisfy the constraint $\mathcal{A}$ and $|e_2| < k_{b2}$, and from inequality (54c), it is derived that $\beta_i \in [-3\pi/180, 3\pi/180]$ $(i = 1, 2)$. By Eq. (9), it is further derived that

$$\sin\beta_1 - \sin\beta_2 = k_2 \frac{e_2}{V} + \frac{\dot{h}_{\mathrm{r}}}{V_{\mathrm{r}} V} e_1.$$

Given that $\dot{h}_{\mathrm{r}}$ is bounded (Assumption 1), V and V_{r} satisfy the constraint $\mathcal{A}$, and $e_i \to 0$ $(i = 1, 2)$, it is clear that $\sin\beta_1 - \sin\beta_2 \to 0$. Because $\beta_i \in [-3\pi/180, 3\pi/180]$ $(i = 1, 2)$, it can be concluded that $\beta_1 - \beta_2 \to 0$. Now, let us consider Eq. (58). According to $e_i \to 0$ $(i = 3, 4)$ and $\beta_1 - \beta_2 \to 0$, it is clear that $\alpha - \alpha_{\mathrm{r}} \to 0$. Hence, we have proved property (iii).

Now, we have completed the proof of the theorem.

In Theorem 1, a set of criteria, i.e., inequalities (53) and (54a)–(54e), is given, providing a guideline for the design of reference trajectories and the selection of control parameters. From inequalities (54a)–(54e), it can be observed that when the reference trajectories are slowly time-varying and they are always far away from the bounds of $\mathcal{A}$, the parameters k_{bi} $(i = 1, 2, \ldots, 5)$ can be selected over a large range. Together with inequality (53), it is further concluded that large initial tracking errors can be accepted. Otherwise, k_{bi} $(i = 1, 2, \ldots, 5)$ can be selected only in a narrow range, which means that the initial tracking errors must be very small.

3.4 Solvability analysis of the controller parameters

In this subsection, let us analyze the solvability of the controller parameters k_i and k_{bj} $(i, j = 1, 2, \ldots, 5)$ in the criteria (inequalities (53) and (54a)–(54e)). We have the following theorem:

Theorem 2 Suppose Assumptions 1–3 hold. If the initial state $\boldsymbol{x}(0)$ and the reference trajectories $\boldsymbol{y}_{\mathrm{r}}(t)$ satisfy the following inequalities:

$$|V(0) - V_{\mathrm{r}}(0)| < \min\{3352.8 - (V_{\mathrm{r}})_{\max}, (V_{\mathrm{r}})_{\min} - 2286\}, \tag{59}$$

$$|h(0)-h_{\rm r}(0)|<\min\{41\,148-(h_{\rm r})_{\max},(h_{\rm r})_{\min}-21\,336\}, \tag{60}$$

$$|\theta_{\rm p}(0)-\theta_{\rm r}(0)|< \min\{7\pi/180-(\theta_{\rm r})_{\max},(\theta_{\rm r})_{\min}-(-2\pi/180)\}, \tag{61}$$

$$\left|\gamma(0)-\arcsin\frac{\dot{h}_{\rm r}(0)}{V(0)}\right|<3\pi/180-\arcsin\frac{(\dot{h}_{\rm r})_{\max}}{2286}, \tag{62}$$

$$|Q(0)-\dot{\theta}_{\rm r}(0)|< \min\{10\pi/180-(\dot{\theta}_{\rm r})_{\max},(\dot{\theta}_{\rm r})_{\min}-(-10\pi/180)\}, \tag{63}$$

then there exist positive constants k_i and k_{bj} ($i,j=1, 2, \ldots, 5$) such that inequalities (53) and (54a)–(54e) hold. In inequalities (59)–(63), the numerical values such as 2286 and 3352.8 are from Table 1.

Proof First, according to inequality (59), k_{b1} is selected as

$$|V(0)-V_{\rm r}(0)|<k_{b1}< \min\{3352.8-(V_{\rm r})_{\max},(V_{\rm r})_{\min}-2286\}, \tag{64}$$

which is equivalent to the following two inequalities:

$$|V(0)-V_{\rm r}(0)|<k_{b1}, \tag{65}$$

$$k_{b1}<\min\{3352.8-(V_{\rm r})_{\max},(V_{\rm r})_{\min}-2286\}. \tag{66}$$

By Eq. (9) and inequality (65), it is derived that

$$|e_1(0)|=|V(0)-V_{\rm r}(0)|<k_{b1}. \tag{67}$$

It is easy to see that inequality (66) is equivalent to the following inequality:

$$2286<(V_{\rm r})_{\min}-k_{b1}<(V_{\rm r})_{\max}+k_{b1}<3352.8. \tag{68}$$

From inequalities (67) and (68), it can be concluded that inequalities (53) (with $s=1$) and (54a) are satisfied.

Second, according to inequality (60), k_{b2} is selected as

$$|h(0)-h_{\rm r}(0)|<k_{b2}< \min\{41\,148-(h_{\rm r})_{\max},(h_{\rm r})_{\min}-21\,336\}.$$

Similar to the analysis of inequalities (64)–(68), it can be concluded that inequalities (53) (with $s=2$) and (54b) are satisfied.

Third, according to inequality (61), k_{b4} is selected as

$$|\theta_{\rm p}(0)-\theta_{\rm r}(0)|<k_{b4}< \min\{7\pi/180-(\theta_{\rm r})_{\max},(\theta_{\rm r})_{\min}-(-2\pi/180)\}.$$

Similar to the analysis of inequalities (64)–(68), it can be concluded that inequalities (53) (with $s=4$) and (54d) are satisfied.

Fourth, according to inequality (62), k_{b3} is selected as

$$\left|\gamma(0)-\arcsin\frac{\dot{h}_{\rm r}(0)}{V(0)}\right|<k_{b3} <3\pi/180-\arcsin\frac{|\dot{h}_{\rm r}|_{\max}}{2286}. \tag{69}$$

By Eqs. (24) and (20), it can be seen that inequality (53) (with $s=3$) is equal to

$$\left|\gamma(0)-\arcsin\frac{-k_2e_2(0)+\dot{h}_{\rm r}(0)}{V(0)}\right|<k_{b3}. \tag{70}$$

Given that k_{b3} satisfies inequality (69), it can be concluded that there exists a sufficiently small positive constant k_2^* such that inequality (70), i.e., inequality (53) with $s=3$, holds for any $0<k_2<k_2^*$. Furthermore, according to inequality (69), it is clear that

$$k_{b3}+\arcsin\frac{|\dot{h}_{\rm r}|_{\max}}{2286}<3\pi/180. \tag{71}$$

From inequality (71), it can be concluded that there exists a sufficiently small positive constant k_2^{**} such that inequality (54c) holds for any $0<k_2<k_2^{**}$. Define $\sigma=\min\{k_2^*,k_2^{**}\}$ and it can be concluded that inequalities (53) (with $s=3$) and (54c) hold for any $0<k_2<\sigma$.

Fifth, according to inequality (63), k_{b5} is selected as

$$|Q(0)-\dot{\theta}_{\rm r}(0)|<k_{b5}< \min\{10\pi/180-(\dot{\theta}_{\rm r})_{\max},(\dot{\theta}_{\rm r})_{\min}-(-10\pi/180)\}. \tag{72}$$

Similar to the analysis of inequalities (69)–(71), it can be concluded that there exists a sufficiently small positive constant μ such that inequalities (53) (with $s=5$) and (54e) are satisfied for any $0<k_4<\mu$.

Finally, choose $k_j>0$ ($j=1,3,5$) arbitrarily because the three parameters are independent of the criteria (inequalities (53) and (54a)–(54e)).

Thus, we have completed the proof of the theorem.

Remark 2 In Theorem 2, inequalities (59)–(63) are called the solvability conditions, providing a guideline for the selection of reference trajectories. Additionally, the proof process of Theorem 2 gives the selection approach of the controller parameters

k_i and k_{bj} $(i, j = 1, 2, \ldots, 5)$. Obviously, the selection of the controller parameters in the proposed approach is easier than that in the existing approaches (Fiorentini *et al.*, 2009; Fiorentini and Serrani, 2012; Li and Meng, 2015) where the selection of the controller parameters is a trial-and-error procedure.

4 Numerical simulation

In this section, simulation results are provided to show the effectiveness of the method proposed in Theorem 1.

Nominal values of inertial parameters and aerodynamic parameters can be found in Parker *et al.* (2007) and Fiorentini (2010). In the simulation, assume that all the uncertain parameters are randomly generated in the parameter set $\mathcal{P}$. The initial value of the parameter estimate $\hat{\boldsymbol{\theta}}_i$ takes the nominal value of $\boldsymbol{\theta}_i$ $(i = 1, 2, 3)$. Initial states are given as follows:

$$V(0) = 2392.68\ \text{m/s},\ h(0) = 26\,212.8\ \text{m},$$
$$\gamma(0) = 0\ \text{deg},\ \alpha(0) = 1.44\ \text{deg},\ Q(0) = 0\ \text{deg/s}.$$

In this simulation we consider a constant dynamic pressure flight. Given the altitude step command $h_{\text{cmd}} = 3962.4$ m, the altitude reference trajectory h_{r} is generated by

$$\begin{aligned} h_{\text{r}} = & \frac{\omega_1^2\omega_2^2}{(s^2 + 2\xi_1\omega_1 s + \omega_1^2)(s^2 + 2\xi_2\omega_2 s + \omega_2^2)} h_{\text{cmd}} \\ & + h_{\text{r}}(0), \\ & h_{\text{r}}(0) = h(0), \end{aligned}$$

where $\omega_1 = 0.03$, $\omega_2 = 0.02$, and $\xi_1 = \xi_2 = 0.95$. Furthermore, the velocity reference trajectory V_{r} is derived from

$$V_{\text{r}}(t) = \left[\frac{2\overline{q}}{\rho_0} \exp\left(\frac{h_{\text{r}}(t) - h_0}{h_{\text{s}}} \right) \right]^{1/2}$$

to maintain a constant dynamic pressure flight. In the above equation, $\rho_0 = 0.0348$ kg/m^3, $h_0 = 25\,908$ m, $h_{\text{s}} = 6510$ m, and $\overline{q}$ is a constant, which is defined as

$$\overline{q} = \overline{q}(0) = \frac{1}{2}\rho_0 \exp\left(-\frac{h_{\text{r}}(0) - h_0}{h_{\text{s}}} \right) V_{\text{r}}^2(0),$$
$$V_{\text{r}}(0) = V(0).$$

The AOA reference trajectory is generated by

$$\begin{aligned} \alpha_{\text{r}} = & \frac{\omega_3^2\omega_4^2}{(s^2 + 2\xi_3\omega_3 s + \omega_3^2)(s^2 + 2\xi_4\omega_4 s + \omega_4^2)} \alpha_{\text{cmd}} \\ & + \alpha_{\text{r}}(0), \\ & \alpha_{\text{r}}(0) = \alpha(0), \end{aligned}$$

where $\omega_3 = 0.03$, $\omega_4 = 0.02$, $\xi_3 = \xi_4 = 0.95$, and $\alpha_{\text{cmd}} = 0.27$ deg.

The controller parameters are given as follows:

$$k_1 = 10,\ k_2 = 5,\ k_3 = 20,\ k_4 = 1,\ k_5 = 20,$$
$$\boldsymbol{\Gamma}_1 = 0.001\boldsymbol{I}_{12},\ \boldsymbol{\Gamma}_2 = 0.75\boldsymbol{I}_{16},\ \boldsymbol{\Gamma}_3 = 0.01\boldsymbol{I}_{10},$$
$$k_{b1} = 20,\ k_{b2} = 20,\ k_{b3} = \pi/180,$$
$$k_{b4} = 0.1\pi/180,\ k_{b5} = 0.25\pi/180.$$

It is easily verified that the criteria (inequalities (53) and (54a)–(54e)) given in Theorem 1 are satisfied. In the simulation, the following limitations on Φ, δ_{e}, and δ_{c} are imposed:

$$0.005 \le \Phi \le 1.5,$$
$$-20\ \text{deg} \le \delta_{\text{e}} \le 20\ \text{deg},$$
$$-20\ \text{deg} \le \delta_{\text{c}} \le 20\ \text{deg}.$$

Figs. 2 and 3 show the tracking performance of the velocity, Figs. 4 and 5 show the tracking performance of the altitude, and Figs. 6 and 7 show the tracking performance of the AOA. From these simulation results, it can be seen that not only the velocity and the altitude, but also the AOA has good tracking performance over the entire flight. Compared with the existing studies (Fiorentini *et al.*, 2009; Sun HF *et al.*, 2013; Zong *et al.*, 2013), the AOA behaves in an expected manner in the proposed approach, which reduces the coupling between the air-breathing engine and the AOA and thus improves the performance of the air-breathing engine.

Clearly, the velocity, the altitude, and the AOA are always within the envelope $\mathcal{A}$ given in Table 1. Figs. 8–10 show the responses of the FPA, the pitch angle, and the pitch rate, respectively, indicating that these states are also always within the envelope

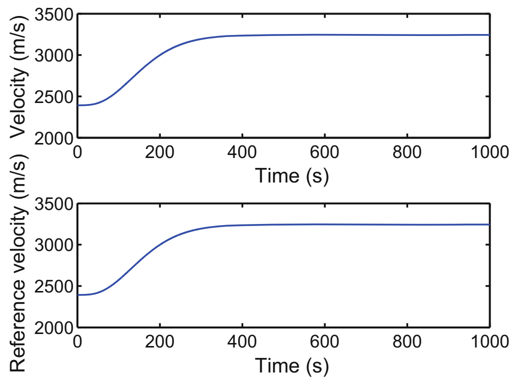

Fig. 2 Velocity tracking

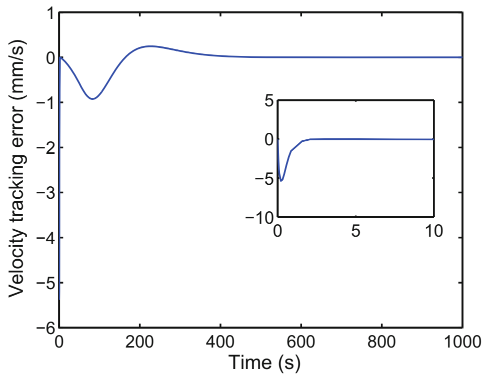

Fig. 3 Velocity tracking error

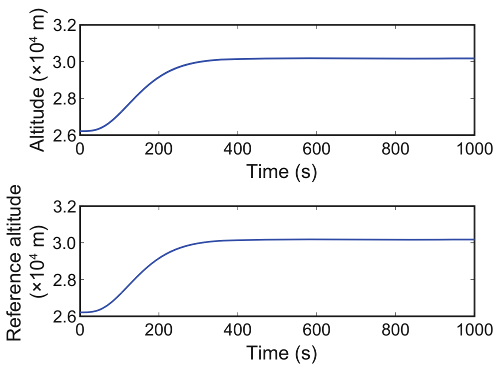

Fig. 4 Altitude tracking

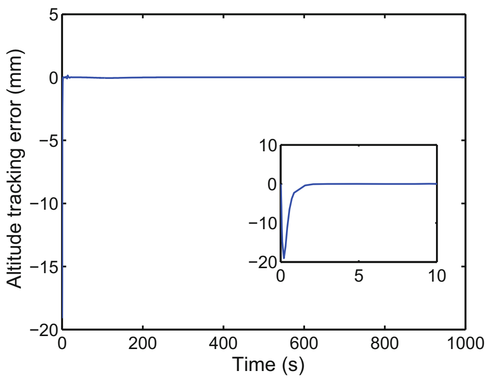

Fig. 5 Altitude tracking error

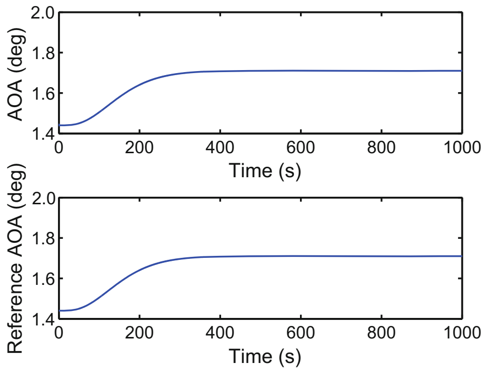

Fig. 6 AOA tracking

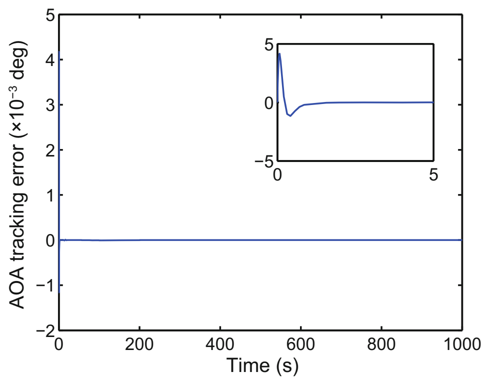

Fig. 7 AOA tracking error

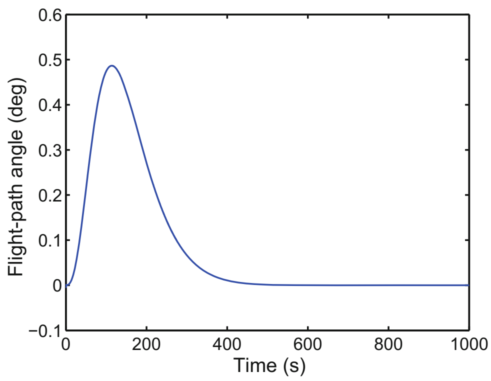

Fig. 8 Flight-path angle

$\mathcal{A}$. In addition, from Figs. 11 and 12, it can be seen that the control inputs satisfy the given constraint. In summary, simulation results test and verify the effectiveness of the proposed approach.

5 Conclusions and future work

We have investigated the tracking problem of the velocity, the altitude, and the AOA for the longitudinal dynamics of air-breathing hypersonic cruise vehicles with state constraints. By redefining the output variables, an indirect AOA tracking strategy has been proposed. Compared with the existing approaches, the proposed approach can not only ensure the tracking of the velocity and the altitude, but also guarantee the tracking of the AOA, which can improve the performance of air-breathing engines. In addition, the conventional barrier Lyapunov function

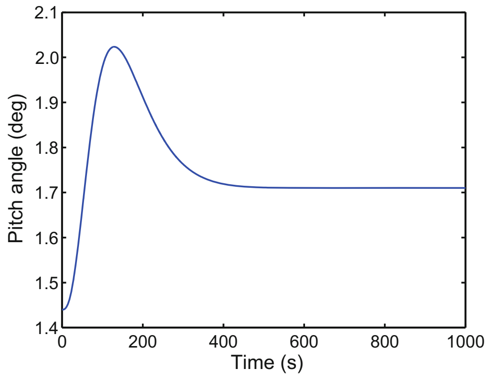

Fig. 9 Pitch angle

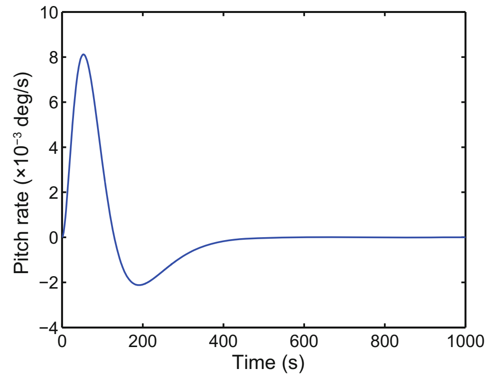

Fig. 10 Pitch rate

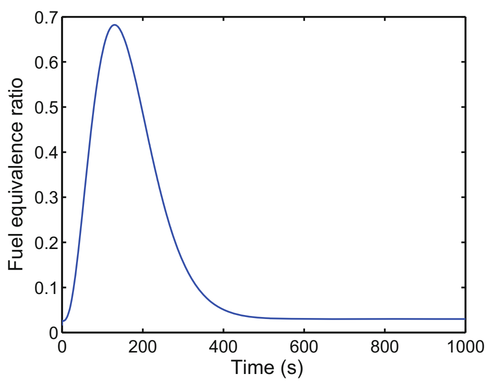

Fig. 11 Fuel equivalence ratio

has been used to solve the state-constrained control problem of the class of systems with unknown control gain, which considerably expands the scope of application of this method. Finally, a set of criteria has been provided, which is simple and can be easily verified. Consequently, the proposed approach greatly simplifies the control design procedure. Simulation results show the effectiveness of the approach.

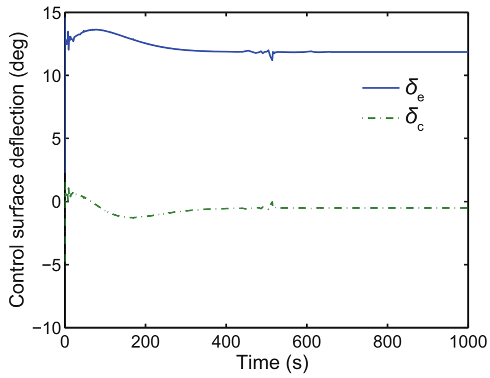

Fig. 12 Control surface deflection

In this paper, the research is focused only on the longitudinal dynamics. These results will be extended to complete six-degree-of-freedom dynamics with flexible modes in future work.

References

Bemporad, A., 1998. Reference governor for constrained nonlinear systems. *IEEE Trans. Autom. Contr.*, **43**(3):415-419. http://dx.doi.org/10.1109/9.661611

Bolender, M.A., Doman, D.B., 2007. Nonlinear longitudinal dynamical model of an air-breathing hypersonic vehicle. *J. Spacecraft Rockets*, **44**(2):374-387. http://dx.doi.org/10.2514/1.23370

Bu, X.W., Wu, X.Y., Ma, Z., *et al.*, 2016. Novel auxiliary error compensation design for the adaptive neural control of a constrained flexible air-breathing hypersonic vehicle. *Neurocomputing*, **171**:313-324. http://dx.doi.org/10.1016/j.neucom.2015.06.058

Burger, M., Guay, M., 2010. Robust constraint satisfaction for continuous-time nonlinear systems in strict feedback form. *IEEE Trans. Autom. Contr.*, **55**(11):2597-2601. http://dx.doi.org/10.1109/TAC.2010.2061090

Cox, C., Lewis, C., Pap, R., *et al.*, 1995. Prediction of unstart phenomena in hypersonic aircraft. Proc. Int. Aerospace Planes and Hypersonics Technologies, Int. Space Planes and Hypersonic Systems and Technologies Conf. http://dx.doi.org/10.2514/6.1995-6018

Fidan, B., Mirmirani, M., Ioannou, P., 2003. Flight dynamics and control of air-breathing hypersonic vehicles: review and new directions. Proc. 12th AIAA Int. Space Planes and Hypersonic Systems and Technologies Conf. http://dx.doi.org/10.2514/6.2003-7081

Fiorentini, L., 2010. Nonlinear Adaptive Controller Design for Air-Breathing Hypersonic Vehicles. PhD Thesis, Ohio State University, USA.

Fiorentini, L., Serrani, A., 2012. Adaptive restricted trajectory tracking for a non-minimum phase hypersonic vehicle model. *Automatica*, **48**(7):1248-1261. http://dx.doi.org/10.1016/j.automatica.2012.04.006

Fiorentini, L., Serrani, A., Bolender, M.A., *et al.*, 2009. Nonlinear robust adaptive control of flexible air-breathing hypersonic vehicles. *J. Guid. Contr. Dyn.*, **32**(2):402-417. http://dx.doi.org/10.2514/1.39210

Gibson, T.E., Crespo, L.G., Annaswamy, A.M., 2009. Adaptive control of hypersonic vehicles in the presence of modeling uncertainties. Proc. American Control Conf., p.3178-3183.
http://dx.doi.org/10.1109/ACC.2009.5160746

Gilbert, E., Kolmanovsky, I., 2002. Nonlinear tracking control in the presence of state and control constraints: a generalized reference governor. *Automatica*, **38**(12):2063-2073.
http://dx.doi.org/10.1016/s0005-1098(02)00135-8

Gregory, I., Mcminn, J., Shaughnessy, J., *et al.*, 1992. Hypersonic vehicle control law development using H_∞ and μ-synthesis. Proc. 4th Symp. on Multidisciplinary Analysis and Optimization Conf.
http://dx.doi.org/10.2514/6.1992-5010

Hu, X., Karimi, H.R., Wu, L., *et al.*, 2014a. Model predictive control-based non-linear fault tolerant control for air-breathing hypersonic vehicles. *IET Contr. Theory Appl.*, **8**(13):1147-1153.
http://dx.doi.org/10.1049/iet-cta.2013.0986

Hu, X., Wu, L., Hu, C., *et al.*, 2014b. Dynamic output feedback control of a flexible air-breathing hypersonic vehicle via T-S fuzzy approach. *Int. J. Syst. Sci.*, **45**(8):1740-1756.
http://dx.doi.org/10.1080/00207721.2012.749547

Jin, X., Kwong, R.H.S., 2015. Adaptive fault tolerant control for a class of MIMO nonlinear systems with input and state constraints. Proc. American Control Conf., p.2254-2259.
http://dx.doi.org/10.1109/ACC.2015.7171068

Krstic, M., Kanellakopoulos, I., Kokotovic, P.V., 1995. Nonlinear and Adaptive Control Design. Wiley.

Li, G.J., Meng, B., 2015. Actuators coupled design based adaptive backstepping control of air-breathing hypersonic vehicle. *IFAC-PapersOnLine*, **48**(28):508-513.
http://dx.doi.org/10.1016/j.ifacol.2015.12.179

Li, S.H., Sun, H.B., Sun, C.Y., 2012. Composite controller design for an airbreathing hypersonic vehicle. *Proc. Instit. Mech. Eng. Part I*, **226**(5):651-664.
http://dx.doi.org/10.1177/0959651811428837

Liu, Y.J., Li, D.J., Tong, S.C., 2014. Adaptive output feedback control for a class of nonlinear systems with full-state constraints. *Int. J. Contr.*, **87**(2):281-290.
http://dx.doi.org/10.1080/00207179.2013.828854

Mayne, D.Q., Rawlings, J.B., Rao, C.V., *et al.*, 2000. Constrained model predictive control: stability and optimality. *Automatica*, **36**(6):789-814.
http://dx.doi.org/10.1016/s0005-1098(99)00214-9

Mirmirani, M., Kuipers, M., Levin, J., *et al.*, 2009. Flight dynamic characteristics of a scramjet-powered generic hypersonic vehicle. Proc. American Control Conf., p.2525-2532.
http://dx.doi.org/10.1109/ACC.2009.5160500

Ngo, K.B., Mahony, R., Jiang, Z.P., 2005. Integrator backstepping using barrier functions for systems with multiple state constraints. Proc. 44th IEEE Conf. on Decision and Control, p.8306-8312.
http://dx.doi.org/10.1109/CDC.2005.1583507

Oland, E., Schlanbusch, R., Kristiansen, R., 2013. Underactuated translational control of a rigid spacecraft. Proc. IEEE Aerospace Conf., p.1-7.
http://dx.doi.org/10.1109/AERO.2013.6497324

Parker, J.T., Serrani, A., Yurkovich, S., *et al.*, 2007. Control-oriented modeling of an air-breathing hypersonic vehicle. *J. Guid. Contr. Dyn.*, **30**(3):856-869.
http://dx.doi.org/10.2514/1.27830

Pettersen, K.Y., 2015. Underactuated marine control systems. *In*: Baillieul, J., Samad, T. (Eds.), Encyclopedia of Systems and Control, p.1499-1503.
http://dx.doi.org/10.1007/978-1-4471-5058-9_125

Qiu, J.B., Feng, G., Gao, H.J., 2013. Static-output-feedback H_∞ control of continuous-time T-S fuzzy affine systems via piecewise Lyapunov functions. *IEEE Trans. Fuzzy Syst.*, **21**(2):245-261.
http://dx.doi.org/10.1109/TFUZZ.2012.2210555

Qiu, J.B., Wei, Y.L., Karimi, H.R., 2015. New approach to delay-dependent H_∞ control for continuous-time Markovian jump systems with time-varying delay and deficient transition descriptions. *J. Franklin Instit.*, **352**(1):189-215.
http://dx.doi.org/10.1016/j.jfranklin.2014.10.022

Qiu, J.B., Ding, S.X., Gao, H.J., *et al.*, 2016. Fuzzy-model-based reliable static output feedback H_∞ control of nonlinear hyperbolic PDE systems. *IEEE Trans. Fuzzy Syst.*, **24**(2):388-400.
http://dx.doi.org/10.1109/TFUZZ.2015.2457934

Serrani, A., 2013. Nested zero-dynamics redesign for a non-minimum phase longitudinal model of a hypersonic vehicle. Proc. 52nd IEEE Conf. on Decision and Control, p.4833-4838.
http://dx.doi.org/10.1109/CDC.2013.6760647

Shaughnessy, J.D., Pinckney, S.Z., McMinn, J.D., *et al.*, 1990. Hypersonic Vehicle Simulation Model: Winged-Cone Configuration. NASA Technical Memorandum 102610, USA.

Slotine, J.J.E., Li, W., 1991. Applied Nonlinear Control. Prentice-Hall Englewood Cliffs, New Jersey, USA.

Sun, H.B., Li, S.H., Sun, C.Y., 2013. Finite time integral sliding mode control of hypersonic vehicles. *Nonl. Dyn.*, **73**(1):229-244.
http://dx.doi.org/10.1007/s11071-013-0780-4

Sun, H.F., Yang, Z.L., Zeng, J.P., 2013. New tracking-control strategy for airbreathing hypersonic vehicles. *J. Guid. Contr. Dyn.*, **36**(3):846-859.
http://dx.doi.org/10.2514/1.57739

Tee, K.P., Ge, S.S., 2011. Control of nonlinear systems with partial state constraints using a barrier Lyapunov function. *Int. J. Contr.*, **84**(12):2008-2023.
http://dx.doi.org/10.1080/00207179.2011.631192

Tee, K.P., Ge, S.S., Tay, E.H., 2009. Barrier Lyapunov functions for the control of output-constrained nonlinear systems. *Automatica*, **45**(4):918-927.
http://dx.doi.org/10.1016/j.automatica.2008.11.017

Wang, T., Gao, H., Qiu, J., 2016. A combined adaptive neural network and nonlinear model predictive control for multirate networked industrial process control. *IEEE Trans. Neur. Netw. Learn. Syst.*, **27**(2):416-425.
http://dx.doi.org/10.1109/TNNLS.2015.2411671

Wolff, J., Weber, C., Buss, M., 2007. Continuous control mode transitions for invariance control of constrained nonlinear systems. Proc. 46th IEEE Conf. on Decision and Control, p.542-547.
http://dx.doi.org/10.1109/CDC.2007.4434916

Wu, H.N., Liu, Z.Y., Guo, L., 2014. Robust L_∞-gain fuzzy disturbance observer-based control design with adaptive bounding for a hypersonic vehicle. *IEEE Trans. Fuzzy Syst.*, **22**(6):1401-1412. http://dx.doi.org/10.1109/TFUZZ.2013.2292976

Xu, B., Gao, D.X., Wang, S.X., 2011. Adaptive neural control based on HGO for hypersonic flight vehicles. *Sci. China Inform. Sci.*, **54**(3):511-520. http://dx.doi.org/10.1007/s11432-011-4189-8

Xu, B., Sun, F., Liu, H., *et al.*, 2012. Adaptive Kriging controller design for hypersonic flight vehicle via back-stepping. *IET Contr. Theory Appl.*, **6**(4):487-497. http://dx.doi.org/10.1049/iet-cta.2011.0026

Xu, H.J., Mirmirani, M.D., Ioannou, P.A., 2004. Adaptive sliding mode control design for a hypersonic flight vehicle. *J. Guid. Contr. Dyn.*, **27**(5):829-838. http://dx.doi.org/10.2514/1.12596

Yang, J., Li, S.H., Sun, C.Y., *et al.*, 2013. Nonlinear-disturbance-observer-based robust flight control for air-breathing hypersonic vehicles. *IEEE Trans. Aerosp. Electron. Syst.*, **49**(2):1263-1275. http://dx.doi.org/10.1109/taes.2013.6494412

Zong, Q., Wang, J., Tao, Y., 2013. Adaptive high-order dynamic sliding mode control for a flexible air-breathing hypersonic vehicle. *Int. J. Robust Nonl. Contr.*, **23**(15):1718-1736. http://dx.doi.org/10.1002/rnc.3040